*Materials Science-Poland, Vol. 27, No. 2, 2009*

# Deposition of Au, Au–V and Au–$VO_x$ on Si wafers by co-sputtering technique

S. NARKSITIPAN[1], T. BANNURU[2], W.L. BROWN[2], R.P. VINCI[2], S. THONGTEM[3*]

[1]Department of Physics, Faculty of Science, Maejo University, Chiang Mai 50290, Thailand

[2]Department of Materials Science and Engineering, Lehigh University, Bethlehem, PA 18015, U.S.A

[3]Department of Physics and Materials Science, Faculty of Science, Chiang Mai University, Chiang Mai 50200, Thailand

Au, Au–V and Au–$VO_x$ thin films were deposited on Si wafers by a co-sputtering technique. A four-point probe shows that the electrical resistivity of pure Au thin film on Si wafer without annealing is 7.2 mΩ·cm. The resistivities of thin films deposited on Si wafers, with or without annealing, tended to increase with the increase in the V and $VO_x$ concentrations, and were attributable to the inhibited drift mobility of charge carriers within the films. By using the nanoindentation technique, the hardness in all cases also tended to increase with the increase in the V and $VO_x$ concentrations. The hardness of pure Au, without annealing, was 2.52 GPa. It decreased to 1.80 GPa and 1.75 GPa after annealing at 200 °C and 400 °C, respectively. SEM and TEM analyses revealed the presence of nanosized particles on the surfaces of the thin films. XRD analysis of Au–4.00% $VO_x$ film deposited on Si wafer detected the presence of Au, VO and Si. However, SAED analysis only detected the presence of Au on the film.

Key words: *Au, Au–V, Au–$VO_x$ thin films; electrical resistivity; hardness*

## 1. Introduction

The development of biological and microelectromechanical systems (MEMS), microelectronics and optoelectronics has been increasingly important, inspiring a number of researchers to investigate new materials for use as thin films [1–3]. Low electrical resistivity, good resistance to wear, and biological compatibility are the prime features of such materials [1, 2]. Among various thin films, Au/Si is widely used due to its chemical stability, low resistivity, good reliability and other factors. These properties, influenced by microstructures and processing temperatures [4], deserve further investigation. Au and its alloys are very attractive for use in many MEMS devices due to

*Corresponding author: schthongtem@yahoo.com; sthongtem@hotmail.com

their low electrical resistivity and good corrosion resistance [1, 2]. Au thin films were deposited on substrates using various methods, such as Au films deposited on glass by ion beam-induced enhanced adhesion [5], nanoparticle Au films by pulsed laser deposition [6], uniform Au film on glass by microwave-assisted deposition [7], Au thin films by Ar sputtering [8] and by thermal evaporation [9], Pt and Au thin films by filtered vacuum arc [10] and Au films by electrodeposition [1]. V is a promising element which can be used as an alloying element of Au [2]. The electrical properties of $VO_x$ are also very attractive. They change between metallic and insulating behaviours, termed metal–insulator transition (MIT) [11, 12]. VO has metallic conductivity due to the overlapping of 3d orbitals of the metal [12]. $VO_2$ exhibits phase change from insulator to metallic state at 68 °C, and $V_2O_5$ does so at 250 °C [11]. $V_2O_3$ undergoes phase transition from semiconductor to metal at –123 °C [13]. It has a low noise property due to its low resistivity at room temperature [13]. Therefore, $VO_x$ film can be used for many applications such as electronic switches, sensors and memory units [11]. The purpose of the research was to deposit Au, Au–V and Au–$VO_x$ thin films on Si wafers by the co-sputtering technique and to investigate their properties.

## 2. Experimental

Au, Au–V and Au–$VO_x$ thin films were deposited on Si wafers by dc magnetron sputtering under the pressure of $4\times10^{-3}$ torr Ar pressure. To deposit the Au–V and Au –$VO_x$ films, two guns were used to control the Au and V compositions. The pressure of $O_2$ equal to $10^{-4}$ Torr was also applied to the Au–$VO_x$ film depositions. Each film was deposited until it was 500 nm thick. A part of the deposited films were subject to annealing at 200 °C and 400 °C for 1 h. In order to characterize the resistivity, hardness, morphology and phase compositions of the deposited films, the following techniques were employed: a four-point probe method, a nanoindentation technique, X-ray diffractometry (XRD), scanning electron microscopy (SEM), transmission electron microscopy (TEM) and selected area electron diffraction (SAED).

## 3. Results and discussion

The electrical resistivities of Au and Au–V thin films deposited on Si wafers (Fig. 1a) increased with the increase in the V concentrations. These observations show that the additional V atoms hindered charged carriers from drifting in the films. The resistivities of pure Au thin films, with or without annealing at 200 °C and 400 °C, share the same values, namely 7.2 mΩ·cm. For the same V concentrations, their resistivities tended to decrease after high temperature annealing, especially at 400 °C. During the annealing, Au and V atoms were arranged in a systematic array, leading to a decrease in resistivity. The resistivities of Au, Au–2.30% $VO_x$ and Au–4.00% $VO_x$ (Fig. 1b), with or without annealing, slowly increased with the increase in the $VO_x$

content, and tended to decrease after the annealing. For each of the annealing temperatures, the resistivity of Au–$VO_x$ is not as great as that of Au–V. The resistivities of Au–4.00% $VO_x$ are almost equivalent to those of the corresponding $VO_x$ –free matrix. They are 17.3 mΩ·cm if the sample is not subject to annealing ($T_R$), whereas it measures 17.7 and 10.2 mΩ·cm if subjected to annealing at 200 °C and 400 °C, respectively.

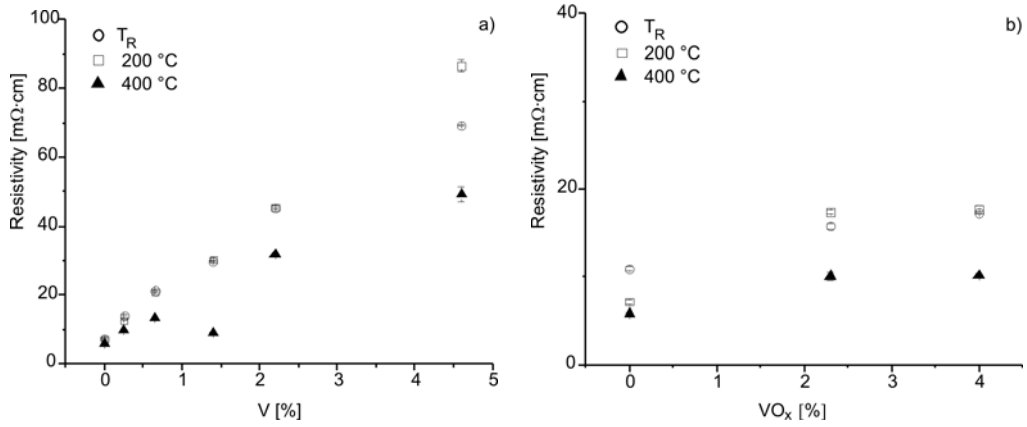


Fig. 1. Resistivities of Au, Au–V (a), and Au–$VO_x$ (b) thin films deposited on Si wafers before (room temperature, $T_R$), and after annealing at 200 °C and 400 °C for 1 h

The hardness of each thin film deposited on Si wafer was measured ten times. Averages and standard deviations have been calculated (Fig. 2). The hardness of various Au and Au–V thin films (Fig 2), with or without annealing, tended to increase with the increase in the V concentrations. The hardness of pure Au not subject to annealing amounted 2.52 GPa, whereas after annealing at 200 °C and 400 °C it was

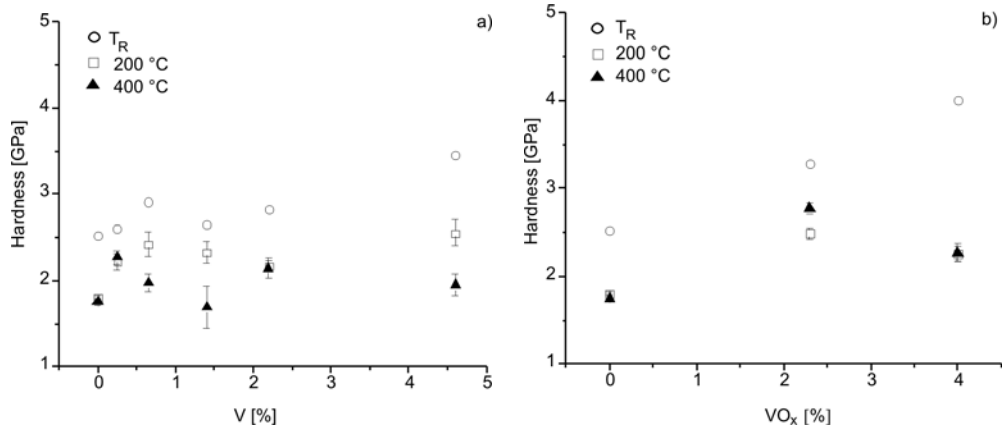


Fig. 2. Hardness values of Au, Au–V (a) and Au–$VO_x$ (b) thin films deposited on Si wafers before and after annealing at 200 °C and 400 °C for 1 h

1.80 GPa and 1.75 GPa, respectively. In comparison with the values obtained for non-annealed films, the hardness of the corresponding thin films deposited on Si wafers became lower after annealing, due to the grain growth and phase change processes. In general, the lowest hardness corresponds to the highest annealing temperature. In the case of Au, Au–2.30% $VO_x$ and Au–4.00% $VO_x$ (Fig. 2b), the hardness also tended to increase with the increase in the $VO_x$ concentration. The greatest hardness, equal to 4.00 GPa, was found in non-annealed Au–4.00% $VO_x$. The higher hardness implies that $VO_x$ particles have the effect of hindering plastic deformation of thin films, by trapping dislocations. The hardness became lower when the films were subject to annealing.

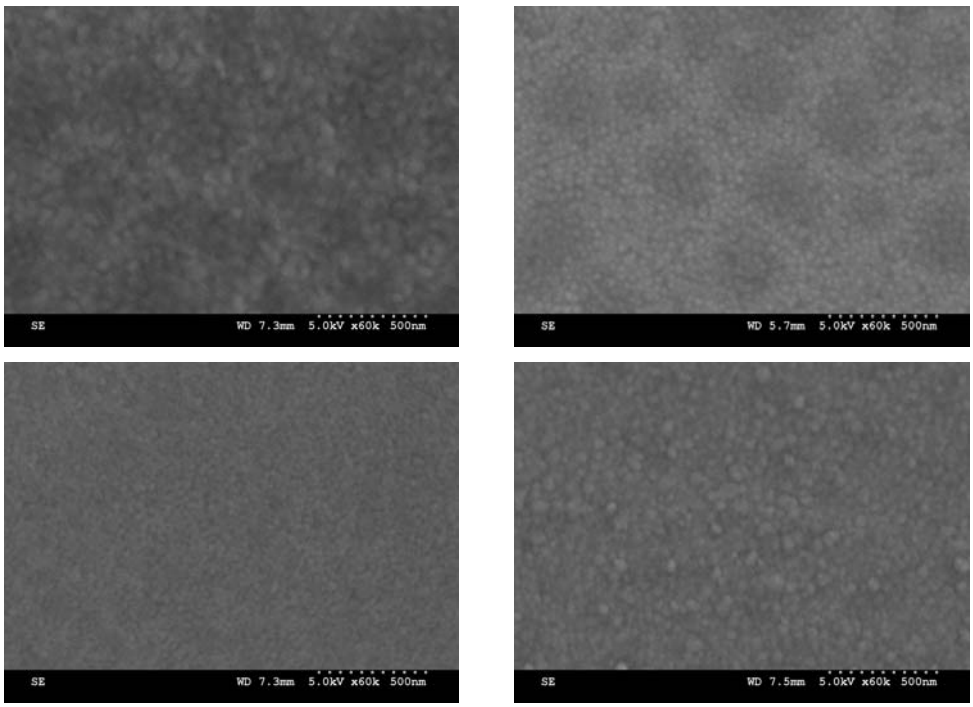


Fig. 3. SEM images of: a) Au, b) Au–0.65% V, c) Au–4.60% V and d) Au–4.00% $VO_x$ thin films deposited on Si wafers after annealing at 200 °C for 1 h

SEM images show general morphologies of the films. After annealing at 200 °C, the Au, Au–0.65% V and Au–4.60% V surfaces (Figs. 3a–c) were composed of a number of nanodots or nanoparticles, although the films did contain a variety of V concentrations. The average size of pure Au particles was 56 nm. The addition of V to Au led to the reduction in their sizes by hindering grain boundary mobility. For the Au–4.00% $VO_x$ surface (Fig. 3d), a number of nanoparticles were also detected. This reflects their properties such as electrical resistivity, surface roughness and hardness.

TEM image data (Fig. 4a) show that the thin film was composed of a number of dispersed, nanosized particles. Different colours (dark, white and gray) appear on the

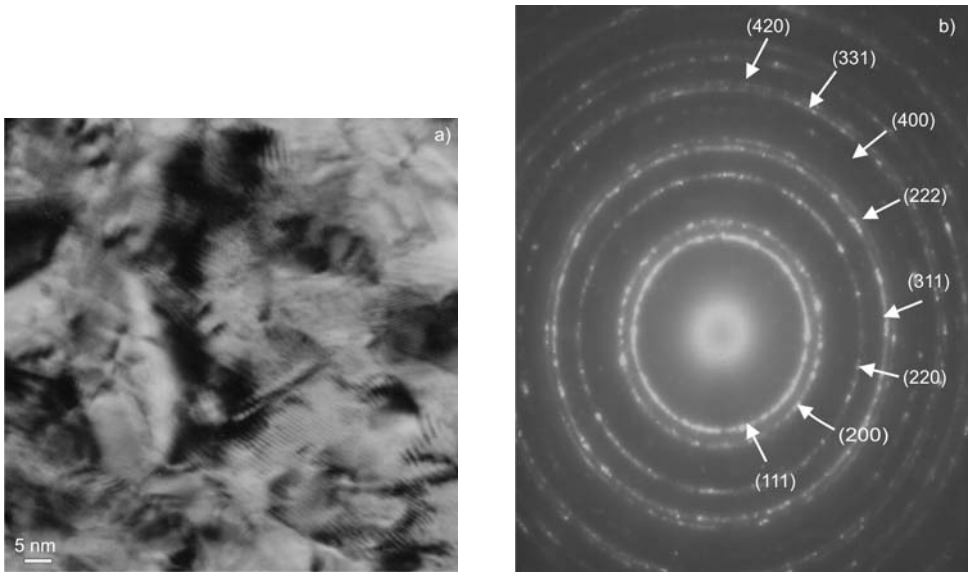


Fig. 4. TEM image (a) and SAED pattern (b) of Au–4.00% $VO_x$ thin film without annealing at a high temperature

image, showing that a rough surface had been produced on the wafer. Moiré fringes were detected. They are the interference patterns of two crystallographic phases with slightly different lattice parameters [14–16]. A SAED pattern (Fig 4b) appears as several concentric rings, due to the diffraction of electrons through the polycrystals. The rings are diffuse and hollow, showing that the thin film was composed of nanosized crystals. Interplanar spaces of the diffraction planes were calculated [17–19] and compared with those computed by the JCPDS software [20]. The pattern corresponds to (111), (200), (220), (311), (222), (400), (331) and (420) planes of the polycrystals, specified as Au (cubic) with *Fm*3*m* space group. The (111) ring has the strongest intensity. No $VO_x$ was detected in the research presented here. Its concentration could have been too low to be detected.

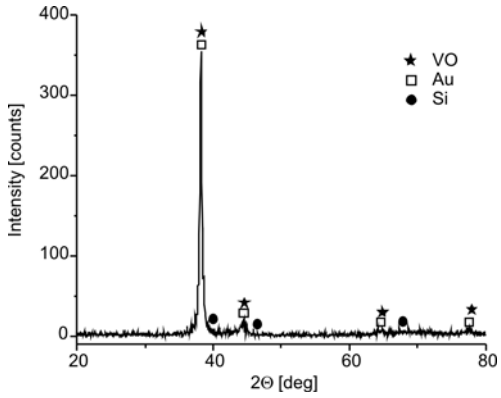


Fig. 5. XRD spectrum of Au–4.00% $VO_x$ thin film deposited on Si wafer without annealing at a high temperature

The XRD spectrum (Fig. 5) was indexed using Bragg's law for diffraction, and was compared with that provided by the JCPDS software [20]. The spectrum is consistent with the deposition of Au and $VO_x$ on Si wafer. It is very sharp, showing that the deposited film was composed of crystals. The strongest intensity peak is at $2\theta = 38.1°$. It mainly diffracted from the (111) plane of Au. VO played a relatively minor role in the diffraction, due to its low concentration (Au–4.00% $VO_x$).

## 4. Conclusions

Au, Au–V and Au–$VO_x$ thin films were successfully deposited on Si wafers using a DC magnetron sputtering technique. The resistivities and hardness of thin films deposited on Si wafer increased with the increase in the V and $VO_x$ concentrations decreased after high temperature annealing. The properties were influenced by the number of nanosized particles and different phases of the thin films.

**Acknowledgement**

We are extremely grateful to the Thailand Research Fund, Thailand, for supporting the research.

## References

[1] KAL S., BAGOLINI A., MARGESIN B., ZEN M., Microelectron. J., 37 (2006), 1329.
[2] LIN M.T., CHROMIK R.R., BARBOSA N. III, EL-DEIRY P., HYUN S., BROWN W.L., VINCI R.P., DELPH T.J., Thin Solid Films, 515 (2007), 7919.
[3] PATRIARCHE G., LE BOURHIS E., FAURIE D., RENAULT P.O., Thin Solid Films 460 (2004), 150.
[4] LEE W.S., FONG F.J., Mater. Sci. Eng. A, 475 (2008), 319.
[5] GUZMAN L., MIOTELLO A., CHECCHETTO R., ADAMI M., Surf. Coat. Tech., 158–159 (2002), 558.
[6] DONNELLY T., KRISHNAMURTHY S., CARNEY K., MCEVOY N., LUNNEY J.G., Appl. Surf. Sci., 254 (2007), 1303.
[7] HUANG H., ZHANG S., QI L., YU X., CHEN Y., Surf. Coat. Tech., 200 (2006), 4389.
[8] DELGADO J.M., ORTS J.M., PÉREZ J.M., RODES A., J. Electroanalyt. Chem., 617 (2008), 130.
[9] ZHANG S., BERGUIGA L., ELEZGARAY J., ROLAND T., FAIVRE-MOSKALENKO C., ARGOUL F., Surf. Sci., 601 (2007), 5445.
[10] SALVADORI M.C., MELO L.L., VAZ A.R., WIEDERKEHR R.S., TEIXEIRA F.S., CATTANI M., Surf. Coat. Tech., 200 (2006), 2965.
[11] LEE J.W., MIN S.R., CHO H.N., CHUNG C.W., Thin Solid Films, 515 (2007), 7740.
[12] RATA A.D., CHEZAN A.R., PRESURA C., HIBMA T., Surf. Sci., 532–535 (2003), 341.
[13] HAN Y.H., CHOI I.H., KANG H.K., PARK J.Y., KIM K.T., SHIN H.J., MOON S., Thin Solid Films, 425 (2003), 260.
[14] THONGTEM T., PHURUANGRAT A., THONGTEM S., Mater. Lett., 60 (2006), 3776.

[15] GNANASEKAR K.I., CATHRINO H.A., JIANG J.C., MRSE A.A., NAGASUBRAHMANIAN G., DOUGHTY D.H., RAMBABU B., Solid State Ion. ,148 (2002), 299.
[16] YU K., ZHAO J., GUO Y., DING X., BALA H., LIU Y., WANG Z., Mater. Lett., 59 (2005), 2515.
[17] ANDREWS K.W., DYSON D.J., KEOWN S.R., *Interpretation of Electron Diffraction Patterns*, Plenum Press, New York, 1971, p. 14.
[18] THONGTEM T., KAOWPHONG S., THONGTEM S., J. Mater. Sci., 42 (2007), 3923.
[19] THONGTEM T., PHURUANGRAT A., THONGTEM S., J. Mater. Sci., 42 (2007), 9316.
[20] Powder Diffract. File, JCPDS Internat. Centre for Diffract. Data, PA 19073-3273, U.S.A., (2001).

*Received 18 August 2008*